



MDTEB, a new fluorescent label for carbohydrate nanomaterial in vivo studies

Jeremiah W. Woodcock · Douglas M. Fox ·
Ilababen Patel · Joy Dunkers ·
Stephan J. Stranick · Jeffrey W. Gilman

Received: 24 May 2022 / Accepted: 15 March 2023 / Published online: 27 May 2023

This is a U.S. Government work and not under copyright protection in the US; foreign copyright protection may apply 2023

Abstract Typical studies of gastral toxicity of nanoparticles are conducted using radio labeling. This tends to be quite expensive and difficult owing to both the required protocols for working with these materials and also the expense of both the chemical reagents and dedicated instrumentation. A possible alternative is fluorescence labeling. Fluorescence is just as sensitive as scintillation, given that scintillation is itself a fluorescence measurement and subject to the same limitations. However, most fluorophores are sensitive to changes in pH and hydrolysis reactions present in most mammalian digestive tracts. Here we report the synthesis of a new pH insensitive and hydrolytically stable fluorophore, 10-(4-(3,5-dichlorophenoxy)phenyl)-2,8-diethyl-5,5-difluoro-1,3,7,9-tetramethyl-5 H-4(14,5(14)-dipyrrolo[1,2-c:2',1'-f][1,3,2] diazaborinine (mDTEB). This fluorophore is based on the high quantum yield Boron-dipyrromethene (BODIPY) fluorescent center and is equipped with a

reactive handle for convenient attachment to polysaccharides. We validate its effectiveness by labelling cellulose nano fibers (CNFs) to produce homogeneously labelled bright nanofibrils for toxicity studies.

Keywords Cellulose · Fluorescence · BODIPY · Fluorescence lifetime · Pharmacokinetic studies

Introduction

Carbohydrate nanomaterials (CNM) have been identified as an important class of compounds in a growing number of applications (Lin et al. 2012; Huang et al. 2014; Kang et al. 2015; Lopez-Lopez et al. 2015; Stine 2015). In particular, they have been identified in many applications that involve potential CNM ingestion, such as in the protection and delivery of bioactive compounds and nutrients (Lin et al. 2012; Huang et al. 2014; Kang et al. 2015; Lopez-Lopez et al. 2015; Stine 2015), bioconjugation of metal nanoparticles for improved biological interfaces (Lin et al. 2012; Huang et al. 2014; Kang et al. 2015; Stine 2015), biosensor design (Lin et al. 2012; Stine 2015), wound dressings (Mincea et al. 2012; Gokarneshan 2017), tissue engineering (Mincea et al. 2012; Huang et al. 2014; Gokarneshan 2017), food coatings and packaging, (Janjarasskul and Krochta 2010; Cazón et al. 2017) and food additives (Neethirajan and Jayas 2011; Dickinson 2012; Kaur et al. 2018). The commercialization of these materials often requires

Supplementary Information The online version contains supplementary material available at <https://doi.org/10.1007/s10570-023-05152-5>.

J. W. Woodcock · J. Dunkers · S. J. Stranick ·
J. W. Gilman (✉)
National Institute of Standards and Technology,
Gaithersburg, MD, USA
e-mail: gilmanjeff@lamtec.com

D. M. Fox · I. Patel
Department of Chemistry, American University,
Washington D.C, USA

knowledge of the absorption, distribution, metabolism, and excretion (ADME) of the material in animals.

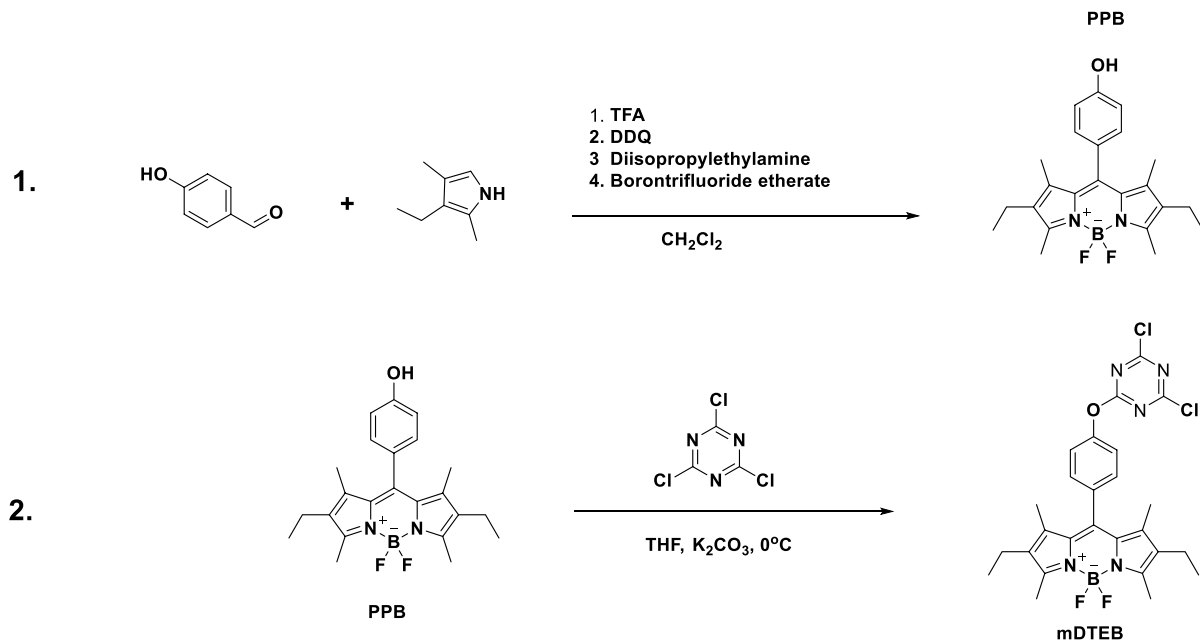
The U.S. Food and Drug Administration (FDA) provides regulatory guidelines on the safety assessment of food ingredients and recommends use of radiolabeled materials for ADME and pharmacokinetic studies, because radiolabels are relatively easy to detect in samples of tissues and body fluids (US FDA 2007). The radiolabel should be uniformly distributed in the molecule and should not be biologically labile. However, radiolabeling carbohydrate nanoparticles is particularly challenging. Cellulose and starch have been labeled by growing plants in radioactive nutrients (Crawford et al. 1977; Benner and Hodson 1985) but that requires subsequent processing of the radioactive material into the nano form. Obtaining the licensing, dedicating the necessary processing equipment, tracking all radioactivity during processing steps, and handling the large amount of radioactive waste are daunting challenges. Labeling the nanomaterials with a small radioactive tag is also challenging, primarily because most carbohydrates must be processed in water to prevent irreversible aggregation of the particles, which would destroy the desired nano-morphology (Dufresne 2013; Visakh and Yu 2016). As an alternative, fluorescent dyes have often been used to track carbohydrate nanoparticles in vivo (Zhao and Wu 2006; Dong and Roman 2007; Nielsen et al. 2010; Li et al. 2011; Zhou et al. 2014; Foster et al. 2018), since they offer the advantages of covalent attachment and detection limits close to that of radiolabels.

There have been many studies that utilized fluorescently labeled carbohydrate nanoparticles (Stine 2015). The use of Rhodamine B derivatives is especially attractive for biological applications because it is relatively photostable, has a high quantum yield, readily penetrates cell membranes, and the excitation and emission bands are red-shifted compared to most auto fluorescing molecules found in nature (Sameiro and Gonçalves 2009; Mottram et al. 2012). However, the quantum yield and attachment chemistries are only stable over a narrow pH range (Shaw and Walker 1958; Sadowski 1978; Bourne et al. 1984; Banks and Paquette 1995; Sahu et al. 2011; Sunasee 2014), leading to challenges in digestive studies where the pH ranges from 1.5 in the stomach to about 9 in the colon. (Xu et al.

2015) Therefore, the only viable (stable) attachment chemistries for digestive studies are amide bonds (Smith and Hansen 1998) and ether bonds (Ranu and Bhar 1996). The amide linkage requires either an amine or a carboxylic acid functionality on the carbohydrate. Although these are present on some polysaccharides, such as chitin, chitosan, and alginate, they are absent on polysaccharides such as cellulose and starch. Amine functionalization of cellulose requires multiple reaction and purification steps, and often significantly changes the surface chemistry of the carbohydrate (Cellulose and Cnc 2019). The ether bond can be formed using fluorescent dyes with dichlorotriazine functionality. These have been used extensively to functionalize nanocellulose (Dong and Roman 2007) and starch (Hong and Huber 2015). However, there are only two that are commercially available: 5-(4,6-Dichlorotriazinyl) aminofluorescein (DTAF) and Texas Red C2-dichlorotriazine (TR). DTAF, which is based on a fluorescein structure is not photostable and the quantum yield is largely dependent on the pH of the medium. TR is much more photo and pH stable, but it has a very low quantum yield. So, there is a need for new hydroxyl-reactive fluorescent dyes to enable reliable ADME and pharmacokinetic studies of polysaccharides.

Boron-dipyrromethene (BODIPY) dyes are a very popular choice for biological applications (Ulrich et al. 2008; Sameiro and Gonçalves 2009; Banuelos-Prieto and Llano 2018). Most BODIPY dyes have high quantum yields, are photostable, have environment-independent quantum yields, are relatively chemically stable, are of low toxicity, and can be structurally modified to generate a desired excitation wavelength. Due to their high stability and great chemical versatility, BODIPY are great candidates for the synthesis of a carbohydrate nanoparticle specific label.

In this study, we report on the synthesis of a new BODIPY dye (mDTEB) designed to chemically attach to polysaccharides and which addresses the issues discussed above. The BODIPY core was modified with ethyl groups (see Scheme 1) to present a chemically stable periphery to aqueous media and to inhibit attacks on the redox sites and the electrophilic sites of the indacene core. The purified product was characterized using solution NMR and fluorescence measurements. The dye was used to label cellulose



Scheme 1 Synthesis of mDTEB: (1) Synthesis of PPB using a one pot, four step synthesis. (2) Reaction of PPB with trichlorotriazine to form mDTEB

nanofibrils (CNFs) which were characterized using fluorescence lifetime imaging microscopy (FLIM).

Experimental

Materials

All reagents were purchased from Sigma Aldrich and used as received except where specified. Methylene chloride was dried using a solvent purification system. Wood based cellulose nanofibrils were obtained from the University of Maine and used as received (AR-CNFs) or autoclaved at 100 °C in base to remove surface lignin fragments (AC-CNFs). The AR-CNFs were extracted from bleached softwood using mechanical grinding and ultra-refining methods. They are supplied as a 3% by mass aqueous slurry and contain 90% dry mass fines with a nominal fiber width of 50 nm and variable lengths of up to several hundred microns. Prior analysis has shown that they have a specific surface energy of 13 m²/g (iGC), surface energies of $g_d = 48$ mJ/m² and $g_{+/-} = 4.5$ mJ/m², surface charge of −35.6 mV (ZP), and a residual lignin

content of 1.60% by mass insoluble lignin and 0.82% by mass soluble lignin (Patel et al. 2021).

Fluorescence lifetime imaging microscopy

FLIM was conducted on a custom build microscope at the National Institute of Standards and Technology (NIST). The excitation was performed using a Ti:Sapphire laser with a pulse width of 140 fs passed through SHG frequency doubling optics that emitted at 514 nm with an average pulse power of 0.5 μW. The sample excitation used an air objective with a numerical aperture of 0.75. The images were collected by raster scanning the laser focus using an X–Y piezo stage. The resulting fluorescence was collected through the same objective and sent to single photon counting modules (Becker and Hickl) for lifetime measurements through a notch filter to remove excitation light. The images were then analyzed using SPCImage NG software package and thresholded at 50 counts to remove background noise. The decay curves were fit using an algorithmically estimated IRF for each pixel. Phasors were generated using the time domain methodology with Eqs. (1 and 2), where $g(\omega)$ and $s(\omega)$ are x and y coordinates of a cartesian

plot. The phasors were then exported and replotted using Origin Pro 2019.

$$S_i(\omega) = \frac{\int_0^\infty I(t)\sin(n\omega t)dt}{\int_0^\infty I(t)dt} \quad (1)$$

$$G_i(\omega) = \frac{\int_0^\infty I(t)\cos(n\omega t)dt}{\int_0^\infty I(t)dt} \quad (2)$$

where ω is the angular repetition frequency of the excitation source; n is the harmonic frequency, $I(t)$ the decay at each time in each pixel.

Dye synthesis

Synthesis of 4-(2,8-diethyl-5,5-difluoro-1,3,7,9-tetra-methyl-5 H-414,514-dipyrrolo[1,2-c:2',1'-f][1,3,2] diazaborinin-10-yl)phenol (PPB)

PPB was synthesized using a modified procedure common to the literature (Baruah et al. 2005). 4-hydroxy benzaldehyde (219.0 mg, 1.79 mmol) and freshly distilled 3-ethyl-2,4-dimethylpyrrole (379.8 mg, 3.42 mmol) were dissolved in 5 mL of methylene chloride under nitrogen atmosphere. One drop of trifluoroacetic acid (TFA) was added and the reaction was stirred for 1.5 h after TLC confirmation of aldehyde consumption. Then, 2,3-dichloro-5,6-dicyano-1,4-benzoquinone (DDQ, 488.0 mg, 2.5 mmol) dissolved in 5 mL methylene chloride was added to the solution through a purged syringe. The reaction was stirred for 1 h. The reaction flask was lowered into an ice bath and equilibrated at 0 °C. Diisopropylethylamine (2.55 g, 17.9 mmol) was added using a purged syringe dropwise and the reaction was stirred for 0.5 h. While still in the ice bath, boron trifluoride etherate (2.32 g, 17.9 mmol) was added dropwise using a syringe, due to the presence of an exotherm. The reaction was stirred for 10 h. The reaction mixture was dispersed in 100 mL methylene chloride and washed three times with 100 mL saturated aqueous sodium bicarbonate, followed by three 100 mL washes with deionized water. The organic layer was dried over anhydrous sodium sulfate. PPB was isolated via column chromatography as a vibrant red solid with silica gel as the stationary phase and

chloroform/ethyl acetate/hexanes (v:v, 1:1:3) solvent as mobile phase in a 25% yield. ¹HNMR: (CDCl₃): δ (ppm) 7.1 (m, 2 H, aromatic), 6.9 (m, 2 H, aromatic), 2.5 (3 H, s, CH₃), 2.3 (4 H, q, CH₂), 2.2 (3 H, s, CH₃), 1.3 (9 H, s, CH₃), 1.0 (3 H, t, CH₃). Mass Spec, +M 396.4.

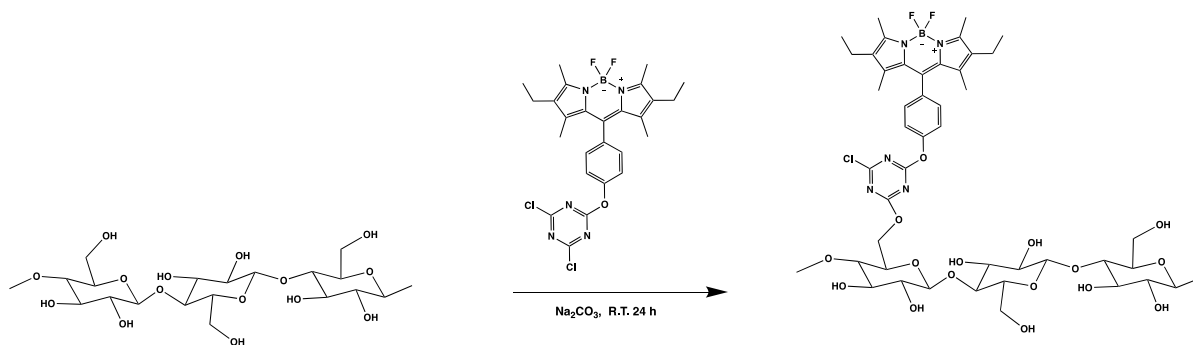
Synthesis of 10-(4-(3,5-dichlorophenoxy)phenyl)-2,8-diethyl-5,5-difluoro-1,3,7,9-tetraethyl-5 H-414,514-dipyrrolo[1,2-c:2',1'-f][1,3,2]diazaborinine (mDTEB)

PPB (10 mg, 18.3 μ mol) and potassium carbonate (10 mg, 72.0 μ mol) were placed in dry THF (2 mL) in a two necked round bottom flask under an argon atmosphere. The flask was lowered into an ice bath and allowed to stir for 30 min. Cyanuric chloride dissolved in dry THF (1 mL) was added using a purged syringe dropwise to the reaction mixture. The reaction was stirred for 10 h. The mDTEB was isolated by column chromatography using acidic alumina as the stationary phase and hexanes/ethylacetate (v:v 1:1) as the mobile phase. The dye structure was confirmed using ¹H NMR and used immediately to functionalize the cellulose. ¹HNMR: (CDCl₃): δ (ppm) 7.2 (m, 2 H, aromatic), 6.6 (m, 2 H, aromatic), 2.5 (3 H, s, CH₃), 2.3 (4 H, q, CH₂), 2.2 (3 H, s, CH₃), 1.3 (9 H, s, CH₃), 1.0 (3 H, t, CH₃).

Cellulose labeling

Attachment of mDTEB to CNF

Cellulose nanofibrils (CNFs with 97 mass% water) from the University of Maine (4.5 g of dry wt.) were added to Na₂CO₃ solution (150 mL 50 mM) and stirred for 30 min. An additional 100 mL of water was added to facilitate stirring. mDTEB (2 mg) was dissolved in 500 μ L of acetone, then added to the alkaline CNF suspension and stirred for 72 h in the dark at room temperature. When the reaction was completed, the modified CNFs were isolated by centrifugation (500 rad/s (5000 rpm) for 20 min). After centrifugation, the excess of mDTEB was removed by washing labeled CNFs with 3 \times 100 mL of an ethyl acetate – water mixture. Purification was carried out using a Speed Mixer (DAC 400 Mixer range, Flack-Tek INC, US) at 157rads/s 1500 rpm for 10 min followed by centrifugation at 4000 rpm for 10 min. The



Scheme 2 mDTEB was dissolved in acetone (4 mg/mL) and added to a stirring dispersion of CNFs in a 1 mmol solution of aqueous sodium carbonate

purification step was repeated until no fluorescent signal was detected in the washing liquor. The CNFs were resuspended in water and repeatedly centrifuged until the ethyl acetate was completely removed. The labeled CNFs were analyzed using a NIST built, time correlated, single photon counting FLIM instrument utilizing a femtosecond Ti-sapphire laser. Samples were excited using 514 nm laser light. An air objective with a numerical aperture of 0.9 was used for imaging. The FLIM images were acquired by building up fluorescence decay curves at each pixel. The decay curve was subsequently fit using a single or multi exponential to determine the lifetime at that pixel. The images presented are $30\ \mu\text{m} \times 30\ \mu\text{m}$ (256 pixels \times 256 pixels) with an integration time of 40 ms/pixel.

Results and discussion

Using the mDTEB discussed above and the method shown in Scheme 2, labelled CNFs were initially prepared using as received CNFs, designated mDTEB-AR-CNFs. Since FLIM is often used to confirm dye-functionalization of biopolymers, it was employed here (Wyatt et al. 1987; Fujimoto et al. 1994; Uversky et al. 1996). Comparison of the data before and after the mDTEB reaction shows very little change in both the FLIM images (Fig. 1D vs. Fig. 1E) or the phasor plots (Fig. 1A vs. Fig. 1B). This is further confirmed by examination of the lifetime distributions shown in Fig. 2, where the distribution peak for the AR-CNFs, from the autofluorescence of lignin on the AR-CNFs, appears similar to the lifetime distribution peak after

treatment with mDTEB (mDTEB-AR-CNFs). We suspected that lignin contained on the AR-CNFs surface was interfering with the cellulose alcohol reaction with mDTEB, and that the lignin was quenching any mDTEB which had attached to either the cellulose or the lignin itself. Studies of the chemical modifications of wood have shown a very high reactivity of the lignin present in the wood (Tjeerdsma and Militz 2005; Iwamoto et al. 2019). This is due to the multiple diverse structures of lignin which are more reactive than the aliphatic alcohols of cellulose. Furthermore, it has been shown that lignin undergoes a self-quenching mechanism (Coletta et al. 2013).

Indeed, autoclave cleaning (105 °C, 15 min, 0.1 M aq NaOH) of the CNFs, which removes the lignin (designated AC-CNFs) and the autofluorescence, followed by reaction with mDTEB did produce the expected enhancement in fluorescence. This is clear from comparison of the FLIM images in Fig. 1F to that in Fig. 1D or Fig. 1E. The successful attachment of mDTEB to the AC-CNFs is further supported by the lifetime distributions shown in Fig. 2, where the peak intensity for mDTEB-AC-CNFs is an order of magnitude greater and the average lifetime is more than doubled (1.5 ns vs. 3.5 ns). In addition, the data for mDTEB-AC-CNF fluorescence lifetime decay curve only requires a single exponential fit, and the phasor plot data for mDTEB-AC-CNFs appears at the universal semicircle at about 3.5 ns (note the tight clustering of the red pixels, Fig. 1C). The single exponential fit and the clustering of the pixels on the universal semicircle is characteristic of fluorophores in very similar environments. In addition, the FLIM image

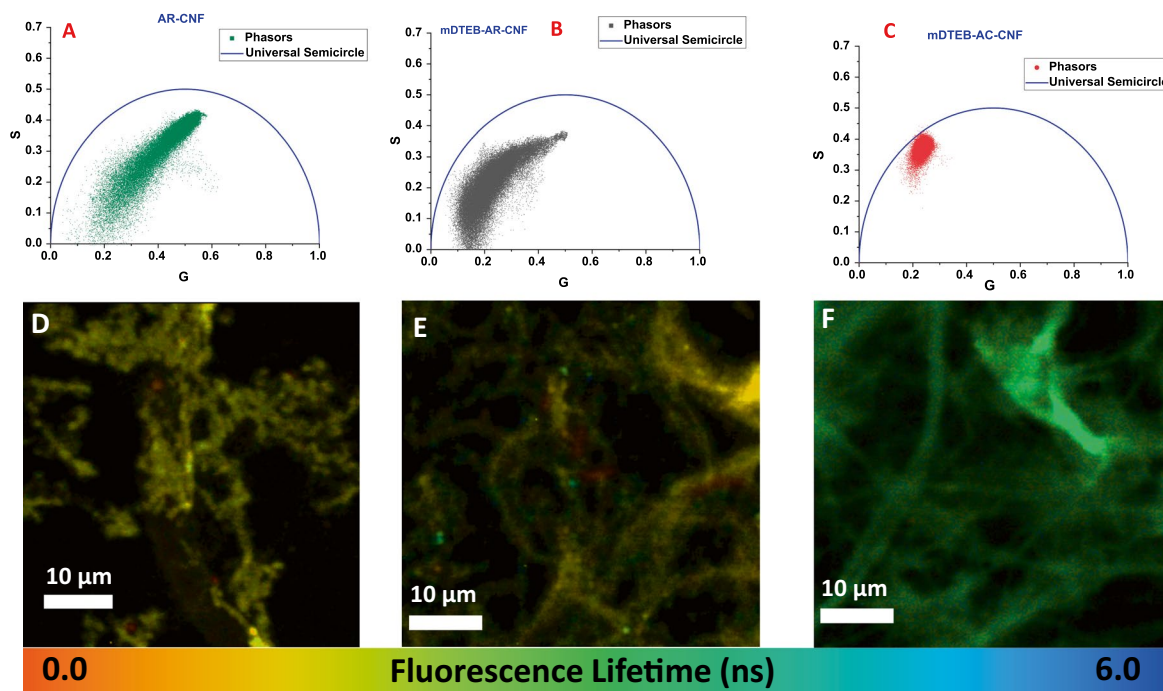


Fig. 1 Phasor plots for as received cellulose nanofibers (A), mDTEB functionalized as received CNFs (B), and autoclaved CNFs labeled with mDTEB (C). False colored fluorescence lifetime maps for as received CNFs (D), mDTEB functional-

ized as received CNFs (E), and autoclaved CNFs functionalized with mDTEB. The false color scale is shown below the images. Images thresholded at 50 counts to remove background noise

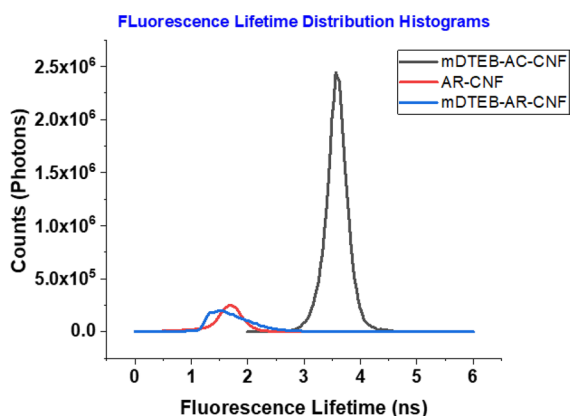


Fig. 2 Average fluorescence lifetime distributions for AR-CNF, mDTEB-AR-CNFs, and mDTEB-AC-CNFs. AR-CNFs and mDTEB-AR-CNFs both required a double exponential fit indicating two component lifetimes (See Figure S.I. 1). mDTEB-AC-CNFs was fit with a single exponential and showed much stronger fluorescence indicating a homogeneous dye environment and covalent attachment

in Fig. 1D of the labeled clean CNFs shows uniform labeling (green color), thus confirming covalent attachment.

The possibility that a large portion of the dye could be removed during ADME or pharmacokinetic studies (i.e., in the biochemical environment mDTEB attached to lignin could be separated from the CNFs) is an additional concern. This would produce erroneous results. To confirm this possibility, we autoclaved the mDTEB-AR-CNFs at pH 13, to produce AC-mDTEB-AR-CNFs (see SI Figure 3a) and found that the sample was no longer fluorescent. However, the same autoclaving of the mDTEB-AC-CNFs produced a sample (AC-mDTEB-AC-CNFs) with persistent fluorescence (see SI Figure 3b). This implies that for AR-CNFs, the mDTEB reacted with surface lignin, rather than the cellulose, and was removed with the lignin during the autoclaving process. It further reinforces the need to label cellulose *after* autoclaving with base treatment to enhance the targeting of cellulose alcohols. Clearly, the impact of the lignin is significant regarding labeling efforts targeted at cellulose.

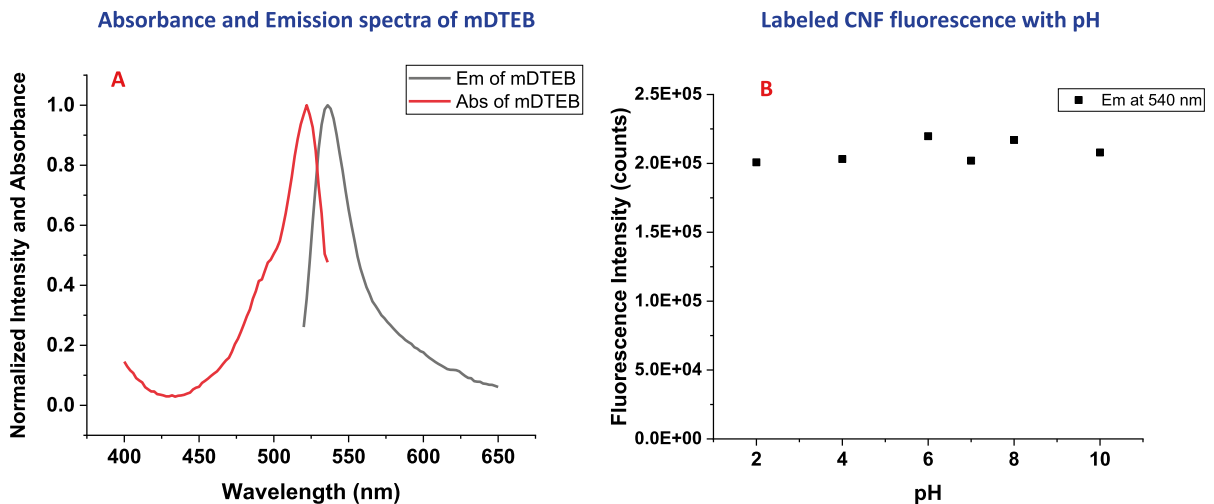


Fig. 3 A. Normalized absorbance spectrum and emission spectrum of mDTEB labeled CNFs in water. Plot of fluorescence intensity as a function of pH for mDTEB labeled CNFs

As mentioned previously, there is a need for pH stable and pH insensitive dyes that can be covalently bound to polysaccharides for ADME and pharmacokinetic studies. This agnostic nature needs also extend to the chemistry binding the dye to the CNF. It is also desirable that these dyes have absorbances and emissions outside that found in biological systems. As can be seen in Fig. 3A, the absorbance peak of mDTEB is at 514 nm with the emission peak at 540 nm. The narrow stoke shift (36 nm) is typical of the Bodipy family of dyes. The alkylation of the core indacene ring structure at the 1, 2, 3, 5, 6 and 7 positions, red shifts the absorbance and emission of the dye and sterically protects the electrophilic centers at these positions. This may also aid in the inhibition of oxidation. To evaluate the pH effect on fluorescence of mDTEB-AC-CNFs the emission intensity of mDTEB labeled CNF was monitored as a function of pH (Fig. 3B). The observed intensity did not vary significantly with changes in pH. The dyed CNFs remained stable at pH values ranging from 2 up to a pH of 10. This is well within the range found in biological settings as well as in the gastral tracts of most mammals.

Conclusions

A new dye was synthesized with a Bodipy core (mDTEB) that is reactive with CNFs, forms an ether type bond with alcohols and is stable to a wide range of pH values. Although used for nanocellulose in this study, it can be used to label a wide range of carbohydrates, including starch, alginates, and dextrans. In addition, the green emission at 540 nm is red shifted from most biologically auto-fluorescing species and is insensitive to pH. The presence of lignin can confound the labeling of cellulose as well as diminish the fluorescence signal from the dye. Removal of surface lignin or lignin fragments prior to labeling is essential for both a durable bond and strong signal. This dye system shows characteristics that make it a great candidate for ADME and pharmacokinetic studies.

Funding The work was done under the auspices of NIST. No external funding contributed to this specific work.

Declarations

Competing interests There are no competing interests known by the authors.

Informed consent Official contribution of the National Institute of Standards and Technology (NIST); not subject to copyright in the United States. Description of commercial products herein is for information only; it does not imply recommendation or endorsement by NIST.

References

- Banks PR, Paquette DM (1995) Comparison of three common amine reactive fluorescent probes used for conjugation to biomolecules by capillary zone electrophoresis. *Bioconjug Chem* 6:447–458. <https://doi.org/10.1021/bc00034a015>
- Banuelos-Prieto J, Llano RS (2018) Introductory chapter: BODIPY dye, and all-in-one molecular scaffold for (Bio) photonics. In: BODIPY Dyes—a privilege molecular scaffold with tunable properties. IntechOpen
- Baruah M, Qin W, Basarić N et al (2005) BODIPY-based hydroxyaryl derivatives as fluorescent pH probes. *J Org Chem* 70:4152–4157. <https://doi.org/10.1021/jo0503714>
- Benner R, Hodson RE (1985) Thermophilic anaerobic biodegradation of [14 C]lignin, [14 C]cellulose, and [14 C] lignocellulose preparations. *Appl Environ Microbiol* 50:971–976. <https://doi.org/10.1128/aem.50.4.971-976.1985>
- Bourne N, Williams A, Douglas KT, Penkava TR (1984) cB mechanism for thiocarbamate Ester. 1827–1832
- Cazón P, Velazquez G, Ramírez JA, Vázquez M (2017) Polysaccharide-based films and coatings for food packaging: a review. *Food Hydrocoll* 68:136–148. <https://doi.org/10.1016/j.foodhyd.2016.09.009>
- Cellulose S, Cnc N (2019) Characterization and cellular internalization of and cancerous fibroblasts. *Materials* 12:3251
- Coletta VC, Rezende CA, Da Conceição FR et al (2013) Mapping the lignin distribution in pretreated sugarcane bagasse by confocal and fluorescence lifetime imaging microscopy. *Biotechnol Biofuels* 6:1–10. <https://doi.org/10.1186/1754-6834-6-43>
- Crawford DL, Crawford RL, Pometto AL (1977) Preparation of specifically labeled 14 C (lignin)- and 14 C (cellulose) lignocelluloses and their decomposition by the microflora of soil. *Appl Environ Microbiol* 33:1247–1251. <https://doi.org/10.1128/aem.33.6.1247-1251.1977>
- Dickinson E (2012) Use of nanoparticles and microparticles in the formation and stabilization of food emulsions. *Trends Food Sci Technol* 24:4–12. <https://doi.org/10.1016/j.tifs.2011.09.006>
- Dong S, Roman M (2007) Fluorescently labeled cellulose nanocrystals for bioimaging applications. *J Am Chem Soc* 129:13810–13811. <https://doi.org/10.1021/ja0761961>
- Dufresne A (2013) Nanocellulose: a new ageless bionanomaterial. *Mater Today* 16:220–227. <https://doi.org/10.1016/j.mattod.2013.06.004>
- Foster EJ, Moon RJ, Agarwal UP et al (2018) Current characterization methods for cellulose nanomaterials. *Chem Soc Rev* 47:2609–2679. <https://doi.org/10.1039/c6cs00895j>
- Fujimoto BS, Clendenning JB, Delrow JJ et al (1994) Fluorescence and photobleaching studies of methylene blue binding to DNA. *J Phys Chem* 98:6633–6643. <https://doi.org/10.1021/j100077a033>
- Gokarneshan N (2017) Role of Chitosan in wound Healing - a review of the recent advances. *Glob J Addict Rehabil Med* 4:555636. <https://doi.org/10.19080/GJARM.2017.03.555637>
- Hong JS, Huber KC (2015) Amylose and amylopectin branch chain reactivity in a model derivatization system. *Carbohydr Polym* 122:437–445. <https://doi.org/10.1016/j.carbpol.2015.01.077>
- Huang J, Chang P, Alain NL (eds) (2014) Polysaccharide-based nanocrystals. Wiley-VCH, Weinheim Germany
- Iwamoto S, Saito Y, Yagishita T et al (2019) Role of moisture in esterification of wood and stability study of ultrathin lignocellulose nanofibers. *Cellulose* 26:4721–4729. <https://doi.org/10.1007/s10570-019-02408-x>
- Janjarasskul T, Krochta JM (2010) Edible packaging materials. *Annu Rev Food Sci Technol* 1:415–448. <https://doi.org/10.1146/annurev.food.080708.100836>
- Kang B, Opatz T, Landfester K, Wurm FR (2015) Carbohydrate nanocarriers in biomedical applications: functionalization and construction. *Chem Soc Rev* 44:8301–8325. <https://doi.org/10.1039/c5cs00092k>
- Kaur J, Kaur G, Sharma S, Jeet K (2018) Cereal starch nanoparticles - a prospective food additive. *Crit Rev Food Sci Nutr* 58:1097–1107
- Li Y, Tan Y, Ning Z et al (2011) Design and fabrication of fluorescein-labeled starch-based nanospheres. *Carbohydr Polym* 86:291–295. <https://doi.org/10.1016/j.carbpol.2011.04.049>
- Lin N, Huang J, Dufresne A (2012) Preparation, properties and applications of polysaccharide nanocrystals in advanced functional nanomaterials: a review. *Nanoscale* 4:3274–3294. <https://doi.org/10.1039/c2nr30260h>
- Lopez-Lopez EA, Hernandez-Gallegos MA, Cornejo-Mazon M, Hernandez-Sanchez H (2015) Polysaccharide-based nanoparticles. *Food Nanoscience and Nanotechnology*. Springer International Publishing, Heidelberg, New York
- Mincea M, Negrulescu A, Ostafe V (2012) Preparation, modification, and applications of chitin nanowhiskers: a review. *Rev Adv Mater Sci* 30:225–242
- Mottram LF, Forbes S, Ackley BD, Peterson BR (2012) Hydrophobic analogues of rhodamine B and rhodamine 101: potent fluorescent probes of mitochondria in living *C. elegans*. *Beilstein J Org Chem* 8:2156–2165. <https://doi.org/10.3762/bjoc.8.243>
- Neethirajan S, Jayas DS (2011) Nanotechnology for the Food and Bioprocessing Industries. *Food Bioproc Tech* 4:39–47. <https://doi.org/10.1007/s11947-010-0328-2>
- Nielsen LJ, Eyley S, Thielemans W, Aylott JW (2010) Dual fluorescent labelling of cellulose nanocrystals for pH sensing. *Chem Commun* 46:8929–8931. <https://doi.org/10.1039/c0cc03470c>
- Patel I, Woodcock J, Beams R et al (2021) Fluorescently labeled cellulose nanofibers for environmental health and safety studies. *Nanomaterials* 11. <https://doi.org/10.3390/nano11041015>
- Ranu BC, Bhar S (1996) Dealkylation of ethers. A review. *Org Prep Proc Int* 28:371–409
- Sadkowsky PJ (1978) Photophysics of the acid and base forms of rhodamine B. *Chem Phys Lett* 57:526–529
- Sahu S, Sahoo PR, Patel S, Mishra BK (2011) Oxidation of thiourea and substituted thioureas: a review. *J Sulf Chem* 32:2011
- Sameiro M, Gonçalves T (2009) Fluorescent labeling of biomolecules with organic probes. *Chem Rev* 109:190–212. <https://doi.org/10.1021/cr0783840>
- Shaw WHR, Walker DG (1958) Kinetic studies of thiourea derivatives. IV. The Methylated Thioureas. *Conclus J Am*

- Chem Soc 80:5337–5342. <https://doi.org/10.1021/ja01553a004>
- Smith RM, Hansen DE (1998) The pH-rate profile for the hydrolysis of a peptide bond. *J Am Chem Soc* 120:8910–8913. <https://doi.org/10.1021/ja9804565>
- Stine KJ (2015) *Carbohydrate nanotechnology*. John Wiley and Sons, Inc, Hoboken, NJ
- Sunasee R (2014) *Chistry of Bioconjugates: synthesis, characterization, and Biomedical Applications*, 9781118359th edn. Wiley Blackwell
- Tjeerdsmas BF, Militz H (2005) Chemical changes in hydrothermal treated wood: FTIR analysis of combined hydrothermal and dry heat-treated wood. *Holz Rohund Werkst* 63:102–111. <https://doi.org/10.1007/s00107-004-0532-8>
- US FDA (2007) Guidance for Industry and other stakeholders toxicological principles for the safety assessment of food ingredients. *Hum Stud* 3:1–286
- Ulrich G, Ziessel R, Harriman A (2008) The chemistry of fluorescent bodipy dyes: versatility unsurpassed. *Angew Chem Int* 47:1184–1201. <https://doi.org/10.1002/anie.200702070>
- Uversky VN, Winter S, Löber G (1996) Use of fluorescence decay times of 8-ANS-protein complexes to study the conformational transitions in proteins which unfold through the molten globule state. *Biophys Chem* 60:79–88. [https://doi.org/10.1016/0301-4622\(96\)00009-9](https://doi.org/10.1016/0301-4622(96)00009-9)
- Visakh PM, Yu L (eds) (2016) *Starch-based blends, composites, and nanocomposites*, 37th edn. Royal society of chemistry, Cambridge
- Wyatt WA, Poirier GE, Bright FV, Hieftje GM (1987) Fluorescence spectra and lifetimes of several fluorophores immobilized on nonionic resins for use in fiber-optic sensors. *Anal Chem* 59:572–576. <https://doi.org/10.1021/ac00131a008>
- Xu F, Yan G, Wang Z, Jiang P (2015) Continuous accurate pH measurements of human GI tract using a digital pH-ISFET sensor inside a wireless capsule. *Meas Lond* 64:49–56. <https://doi.org/10.1016/j.measurement.2014.12.044>
- Zhao J, Wu J (2006) Preparation and characterization of the fluorescent Chitosan nanoparticle probe. *Chin J Anal Chem* 34:1555–1559
- Zhou J, Butchosa N, Jayawardena HSN et al (2014) Glycan-functionalized fluorescent chitin nanocrystals for biorecognition applications. *Bioconjug Chem* 25:640–643 <https://doi.org/10.1021/bc500004c>

Publisher's Note Springer Nature remains neutral with regard to jurisdictional claims in published maps and institutional affiliations.